PNAS RESEARCH ARTICLE | EARTH, ATMOSPHERIC, AND PLANETARY SCIENCES

Novel sulfur isotope analyses constrain sulfurized porewater fluxes as a minor component of marine dissolved organic matter

Alexandra A. Phillips[a,1,2], Margot E. White[b], Michael Seidel[c], Fenfang Wu[a], Frank F. Pavia[a], Preston C. Kemeny[a], Audrey C. Ma[d], Lihini I. Aluwihare[b], Thorsten Dittmar[c,e], and Alex L. Sessions[a]

Edited by François Morel, Princeton University, Princeton, NJ; received June 19, 2022; accepted September 2, 2022

Marine dissolved organic matter (DOM) is a major reservoir that links global carbon, nitrogen, and phosphorus. DOM is also important for marine sulfur biogeochemistry as the largest water column reservoir of organic sulfur. Dissolved organic sulfur (DOS) can originate from phytoplankton-derived biomolecules in the surface ocean or from abiotically "sulfurized" organic matter diffusing from sulfidic sediments. These sources differ in $^{34}S/^{32}S$ isotope ratios ($\delta^{34}S$ values), with phytoplankton-produced DOS tracking marine sulfate (21‰) and sulfurized DOS mirroring sedimentary porewater sulfide (~0 to −10‰). We measured the $\delta^{34}S$ values of solid-phase extracted (SPE) DOM from marine water columns and porewater from sulfidic sediments. Marine DOM_{SPE} $\delta^{34}S$ values ranged from 14.9‰ to 19.9‰ and C:S ratios from 153 to 303, with lower $\delta^{34}S$ values corresponding to higher C:S ratios. Marine DOM_{SPE} samples showed consistent trends with depth: $\delta^{34}S$ values decreased, C:S ratios increased, and $\delta^{13}C$ values were constant. Porewater DOM_{SPE} was ^{34}S-depleted (~-0.6‰) and sulfur-rich (C:S ~37) compared with water column samples. We interpret these trends as reflecting at most 20% (and on average ~8%) contribution of abiotic sulfurized sources to marine DOS_{SPE} and conclude that sulfurized porewater is not a main component of oceanic DOS and DOM. We hypothesize that heterogeneity in $\delta^{34}S$ values and C:S ratios reflects the combination of sulfurized porewater inputs and preferential microbial scavenging of sulfur relative to carbon without isotope fractionation. Our findings strengthen links between oceanic sulfur and carbon cycling, supporting a realization that organic sulfur, not just sulfate, is important to marine biogeochemistry.

dissolved organic matter | dissolved organic sulfur | stable isotopes | marine sulfur cycle | sulfurization

Significance

Marine dissolved organic matter (DOM) is a vast reservoir of enigmatically old carbon with important connections to the global carbon cycle and climate. Previous work hypothesized that highly recalcitrant, "sulfurized" organic matter from sulfidic sediments could potentially account for this long-lived carbon. To quantify the contribution of this source, we made sulfur isotope measurements of marine DOM, measuring samples across the Pacific and Atlantic Oceans as well as from the porewaters of sulfidic sediments. We found $\delta^{34}S$ values and C:S ratios that were consistent with ~8% contribution of this abiotic source and conclude that these sulfurized porewater fluxes are not a main component of oceanic DOM budgets.

Dissolved organic matter (DOM) is the largest inventory of fixed carbon in the ocean (~662 Pg carbon) and is a critical component of marine food webs and nutrient cycling (1). DOM has been hypothesized to impact climate over geological time scales via carbon sequestration (1), as a highly recalcitrant subset of DOM persists for many thousands of years, surviving multiple mixing cycles of the ocean for poorly understood reasons (2–4). Therefore, despite decades of intensive study, fundamental questions remain regarding DOM sources and sinks in the modern ocean.

Ksionzek et al. demonstrated that solid-phase extracted DOM (DOM_{SPE}) contains a substantial quantity of organic sulfur (5). The marine dissolved organic sulfur (DOS) pool is estimated to contain ~7 Pg sulfur, more than 10 times that in phytoplankton, bacteria, and particulate organic sulfur (POS) combined (6). Although estimates of DOS concentration vary (5, 7), it is nevertheless clear that DOS is central to marine sulfur cycling (6), with growing evidence for important links to carbon cycling. For example, reduced sulfur compounds within DOS lower trace metal availability by tightly binding free zinc and copper and potentially limiting primary production (8). Concentrations of alkyl thiols, such as the amino acid cysteine, have been correlated to chlorophyll concentrations, implying further connections to phytoplankton growth (9, 10). DOS metabolites may also limit the growth of some marine heterotrophs, as clades of the ubiquitous SAR11 and SAR86 bacteria are unable to assimilate sulfate and must rely on scavenging reduced OS from the water column (11, 12). It remains unknown whether this subset of S-containing molecules (i.e., DOS) within DOM behaves similarly to the larger dissolved organic carbon (DOC) pool or has unique origins and/or dynamics.

A first-order question regarding DOS dynamics is the origin of the organic compounds (Fig. 1). Ksionzek et al. proposed a DOS cycle that mirrors DOC, with DOS produced mainly by phytoplankton in the sunlit ocean. Under this hypothesis, microbial reworking during the aging of DOS, such as heterotrophic uptake for growth or remineralization back to sulfate, leaves remaining DOS compounds increasingly recalcitrant.

Author contributions: A.A.P. and A.L.S. designed research; A.A.P., M.E.W., M.S., F.F.P., P.C.K., L.I.A., and T.D. performed research; A.A.P., F.W., and A.L.S. contributed new reagents/analytic tools; A.A.P., F.W., A.C.M., and A.L.S. analyzed data; and A.A.P., M.E.W., M.S., L.I.A., T.D., and A.L.S. wrote the paper.

The authors declare no competing interest.

This article is a PNAS Direct Submission.

[1]Present address: Earth Sciences Department, University of California Santa Barbara, Santa Barbara, CA 93016.

[2]To whom correspondence may be addressed. Email: phillips.alexandra.a@gmail.com.

This article contains supporting information online at http://www.pnas.org/lookup/suppl/doi:10.1073/pnas.2209152119/-/DCSupplemental.

Published October 6, 2022.

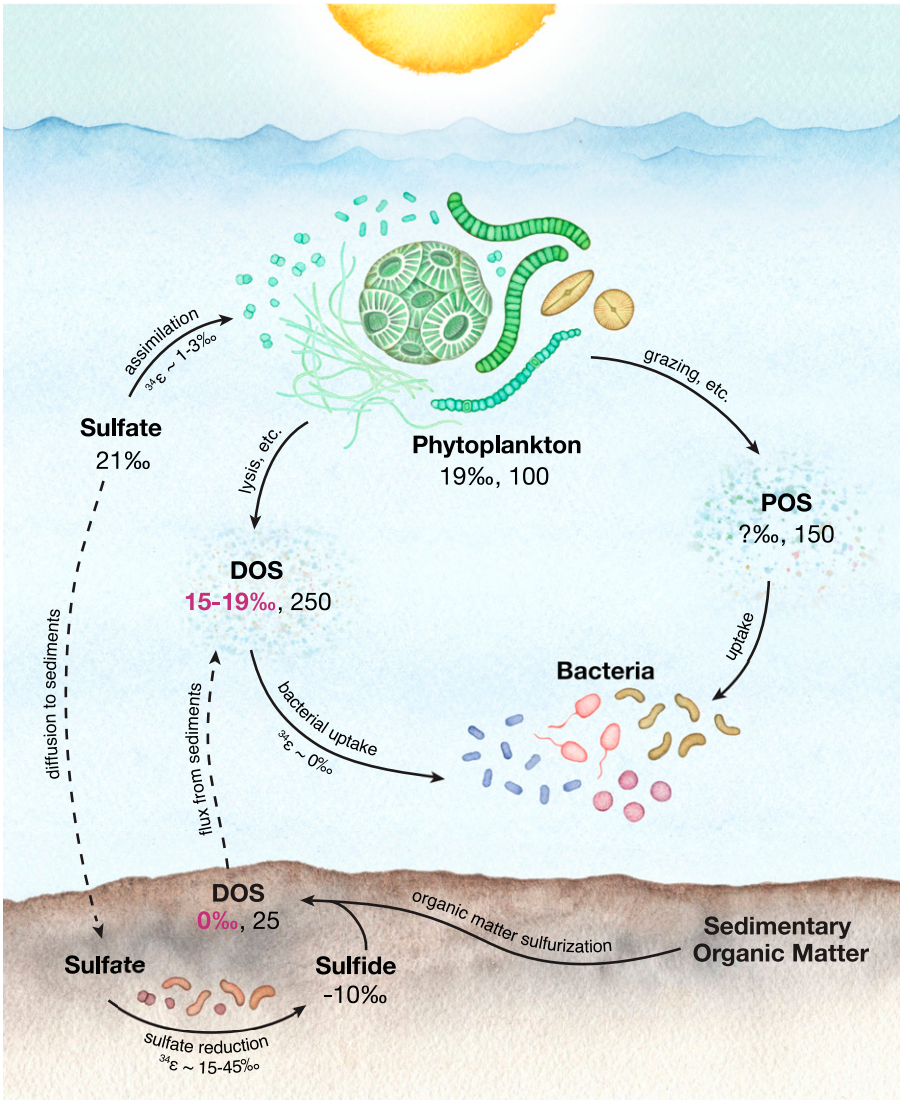

Fig. 1. A simplified marine organic sulfur cycle highlighting processes that may impact the sulfur isotope composition and sulfur content of dissolved organic sulfur (DOS). Numbers underneath each reservoir give the approximate $\delta^{34}S$ value and molar C:S ratio, based on initial studies of organic sulfur in phytoplankton (39, 40), water column DOS (5), and particulate organic sulfur (POS) (42–44), porewater DOS (13), and porewater sulfides (54). Results from this study are highlighted in pink. Through lysis, exudation, and senescence, phytoplankton biomass enters the DOS pool. DOS may also originate from sediments, where sulfide is incorporated into sedimentary organic matter to form sulfurized DOS. The sulfur isotopic composition of DOS_{SPE} indicates the relative balance of these two sources.

DOS may therefore offer a unique lens to DOM cycling more broadly (5). A second hypothesis by Pohlabeln et al. posits that a significant portion of DOS originates in euxinic sediments (13). Here, sulfide produced via microbial sulfate reduction reacts abiotically with organic molecules to "sulfurize" organic matter (14–16). The resulting covalent C-S bonds are thought to be resistant to microbial degradation as a result of stable S-S crosslinking and replace otherwise more labile functional groups (17–19). As such, sulfurization reactions have been recognized as an important pathway for sedimentary organic matter preservation (20–22) and implicated in the carbon cycles of the ancient ocean (e.g., during ocean anoxic events (20, 23)). In modern euxinic sediments, these reactions are a major process: in a study of sedimentary porewater from the Santa Barbara Basin, 70% of detected DOS_{SPE} formulas were products of sulfide and polysulfide sulfurization reactions (24). Pohlabeln et al. calculated the flux of these highly recalcitrant DOS species as a significant source to benthic DOS_{SPE} and by extension to water column DOM_{SPE} (13). While the proportion of DOM molecules that contain sulfur is not known precisely, estimates from molecular formulas of SPE DOM imply it could be ~5–10% (7). Such numbers suggest that porewater-sourced, sulfurized molecules could represent an overlooked subcycle within DOM and might also help to explain why some components of DOM_{SPE} have surprisingly long lifetimes, clarifying connections between DOC and DOS cycles in the ocean (25).

The sulfur isotopic composition of DOS_{SPE} can distinguish between organic matter produced by phytoplankton or by porewater reactions because these sources differ in $\delta^{34}S$ values by ~30‰ (Fig. 1). This signal is easily resolved given typical measurement errors on organic sulfur of ± 0.2‰ (26). Although carbon and nitrogen isotopic measurements have previously proven useful for studying marine DOM_{SPE} (e.g., (27)), to our knowledge, no such measurements have been made for sulfur, likely for two reasons. First, dissolved inorganic sulfate, at 28 mM, is 4–5 orders of magnitude higher in concentration than DOS_{SPE} (~100 nM). To isolate organic sulfur compounds from this high salt background, studies rely on SPE on a styrene-divinylbenzene stationary phase (Bond Elute PPL (28)) that is considered to impart negligible isotope fractionations for

organic compounds (29–31) and should be negligible for sulfur atoms that do not participate in hydrophobic binding interactions. For example, hydrophobic separation of volatile organic sulfur compounds by gas chromatography does not yield fractionation of sulfur isotopes across peaks (32). PPL resins isolate DOM with moderate yields for DOC (~60%), low (~21%) yields for DON, and unknown yields for DOS (33). However, given that abiotically sulfurized organic matter typically has sulfhydryl groups and hydrophobic hydrocarbon regions (24), and given the associated mechanism of retention on SPE columns, PPL should be well suited for retention of sulfurized DOM. Indeed, in a study of dozens of model organic sulfur compounds, extraction efficiency was highest for uncharged, slightly polar, medium-sized analytes (34). Furthermore, both experimentally sulfurized organic matter (13) and sulfurized organic matter from euxinic sediments (24) have been shown to be retained on PPL resins for molecular characterization. We therefore expect $\delta^{34}S$ ratios and C:S ratios of DOS_{SPE} to preferentially retain sulfurized components of bulk DOM. Here, we show that SPE also reduces sulfate contamination to nondetectable levels, allowing accurate isotopic measurements of DOS_{SPE}. The second problem is that conventional isotope ratio mass spectrometry (IRMS) methods have required much more sulfur (~70 μg) than carbon (~20 μg). Given that DOM_{SPE} has high C:S ratios (~150–300), traditional techniques would require extraction from hundreds of liters of seawater per measurement. Recent developments in combustion elemental analysis IRMS (EA-IRMS) have enabled much lower sample sizes (1-10 μg sulfur (26)) for organic sulfur compounds. Here, we used the SPE method and adapted our EA-IRMS measurements to allow simultaneous determination of $\delta^{13}C$ and $\delta^{34}S$ values, and C:S molar ratios on samples of ~350 μg DOM_{SPE}. We applied this approach to extracts from the Pacific and Atlantic coastal zones and ocean basins, generating profiles of $\delta^{34}S$ values of marine DOM_{SPE}. Our data indicate that porewater sulfurization reactions contribute minimally to the marine DOS_{SPE} pool, and by extension, DOS and DOM.

Results

A global sample suite of 90 marine, five estuarine, and five porewater DOM_{SPE} samples were analyzed for $\delta^{13}C$ and $\delta^{34}S$ values, and C:S molar ratios (Fig. 2*A* and *SI Appendix*, Table S1). Samples spanned gyres, shelves, restricted basins, oxygen minimum zones (OMZs), and coastal oceans.

Porewater and Estuary Samples. Porewater DOM_{SPE} was analyzed from sulfidic sediments in the back barrier tidal flats of the North Sea, yielding a $\delta^{34}S$ value of –0.2‰, C:S molar ratio of 18, and $\delta^{13}C$ value of –23.3‰. Meanwhile, porewater DOM_{SPE} samples from sulfidic sediments in the mangrove tidal creek within the Caeté Estuary ranged in $\delta^{34}S$ values from –2.7 to 0.7‰, with C:S molar ratios between 40 and 45 (Fig. 2*B*) and $\delta^{13}C$ values between –27.1 and –26.8‰. DOM_{SPE} surface water samples from the Caeté Estuary were analyzed across a transect from the coastal ocean to the mangrove-fringed estuary. C:S ratios ranged from 74 to 117, with $\delta^{34}S$ values between 4.2 and 8.7‰. $\delta^{13}C$ values spanned –28.6 to –24.2‰ across the transect.

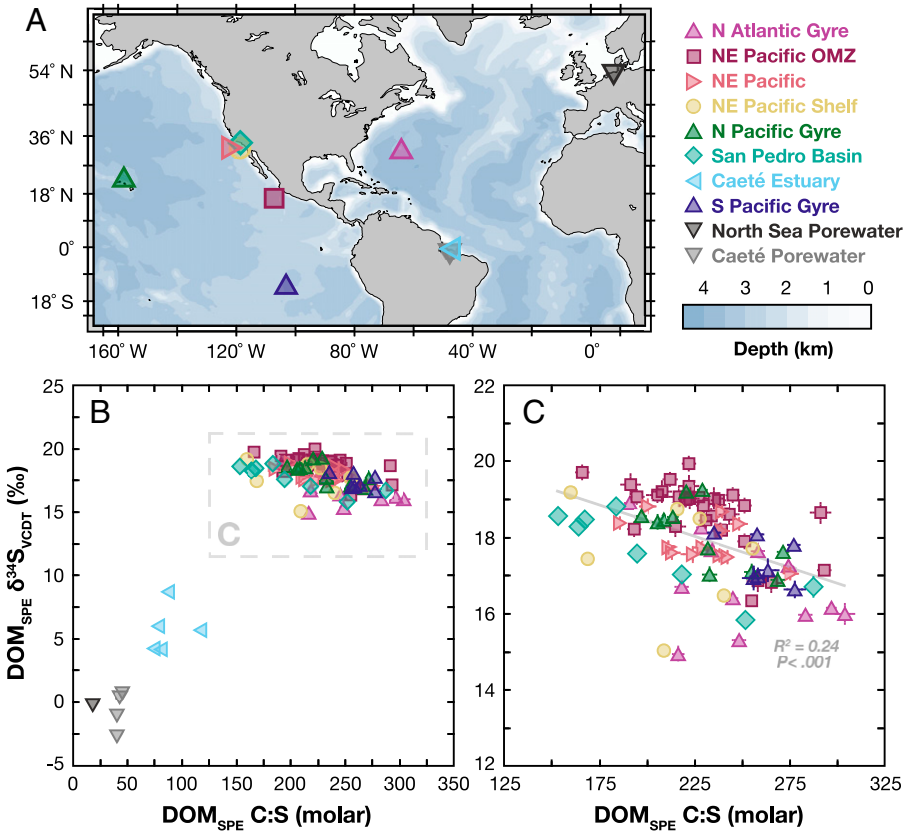

Fig. 2. (*A*) Sample locations spanned gyres (N Atlantic: pink triangles, N Pacific: green triangles, S Pacific: dark blue triangles), shelves (NE Pacific Shelf: yellow circles), mangrove-fringed estuaries (Caeté Estuary: light blue left-facing triangles), restricted hypoxic basins (San Pedro Basin: turquoise diamonds), oxygen minimum zones (NE Pacific OMZ: magenta squares), coastal settings (NE Pacific: light pink right-facing triangles), and sulfidic porewater (North Sea: dark gray down-facing triangles). (*B*) $\delta^{34}S$ values against C:S ratios of all analyzed DOM_{SPE} samples (n = 100). (C) Expanded view of marine DOM_{SPE} samples, showing a negative correlation between DOM_{SPE} $\delta^{34}S$ values and C:S ratios (R^2 = 0.24, P < 0.001). 1σ SEs are shown for all samples in (*B*) and (C), but in many cases, are within the size of the symbol. VCDT, Vienna Canyon Diablo Troilite.

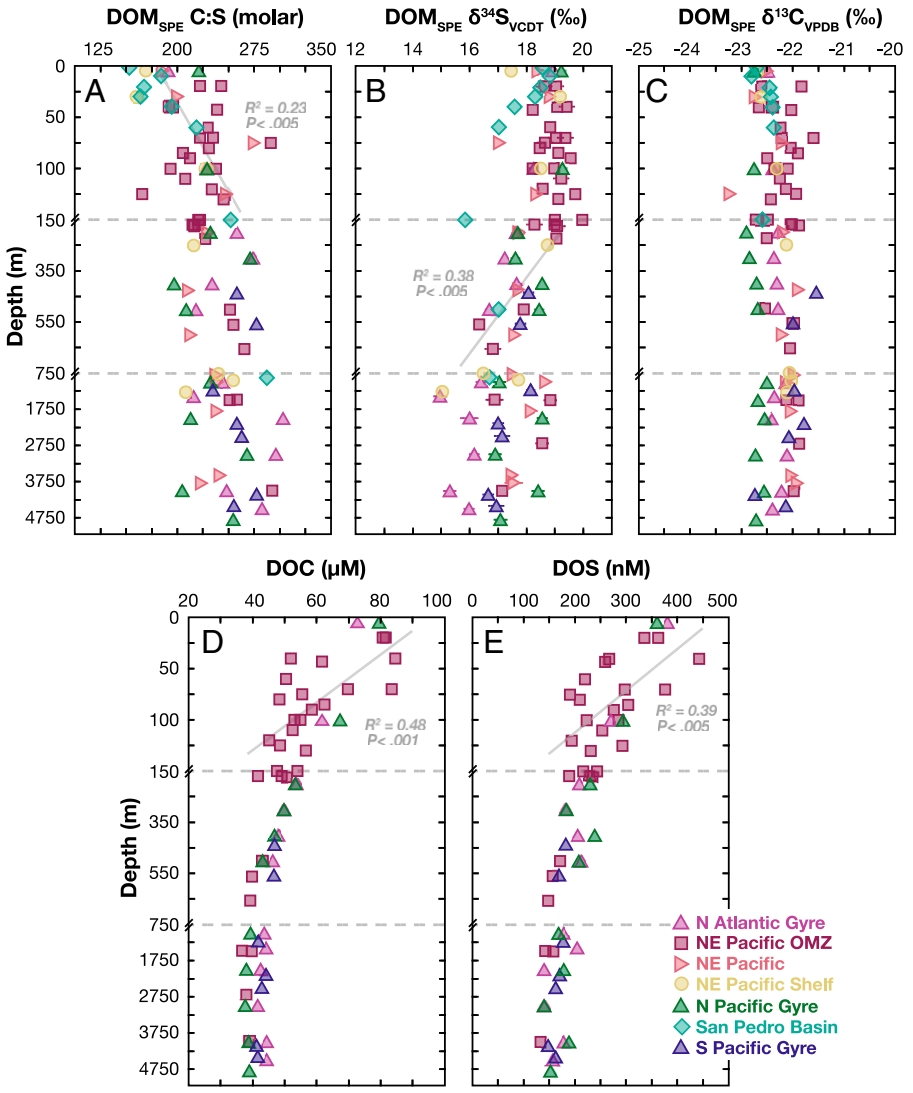

Fig. 3. DOM$_{SPE}$ properties plotted against depth for (*A*) C:S ratios, (*B*) δ^{34}S values (*C*) δ^{13}C values, (*D*) DOC concentration, and (*E*) calculated DOS concentration. Note the scale breaks at 150 m, 750 m on the *y* axis. Colors and symbols for stations are the same as in Fig. 2; significant correlations are marked in gray. 1σ SEs are shown for δ^{34}S values, but error bars for C:S, δ^{13}C values, DOC, and DOS are within the size of the symbol. DOM$_{SPE}$ C:S ratios slightly increased with depth in the first 150 m, but did not change significantly between 150 and 5,000 m. δ^{34}S values averaged 18.6‰ in the first 150 m and decreased between 150 and 750 m to an average of 17.1‰. DOM$_{SPE}$ δ^{13}C values did not change systematically with depth. Both DOC and DOS concentrations decreased within the first 150 m, but did not vary further with depth. For station-specific plots, see *SI Appendix* (*SI Appendix*, Figs. S8, S9, S11–S14).

Marine Samples. Marine DOM$_{SPE}$ ranged in δ^{34}S values from 15 to 20‰ and in molar C:S from 150 to 300. We recognized three distinct behaviors over different depth intervals for DOM$_{SPE}$ measurements, across all sampling locations (Fig. 3 and Table 1). For the purpose of calculating quantitative statistics, we chose typical cutoffs for epipelagic (150 m) and bathypelagic (750 m) zones, while recognizing that such sharp boundaries are somewhat arbitrary and may vary throughout the world's oceans. In the epipelagic shallow samples between 0 and 150 m , C:S ratios of DOM$_{SPE}$ increased (R^2 = 0.23; P < 0.005), resulting in DOC (R^2 = 0.48; P < 0.001) and apparent (see *Materials and Methods*) DOS$_{SPE}$ concentrations (R^2 = 0.39; P < 0.005) that decreased sharply with depth, and δ^{34}S and δ^{13}C values did not change significantly. Average δ^{34}S values and C:S ratios were 18.6 ± 0.8‰ and 213 ± 32, respectively, in this interval. At mesopelagic depths, between 150 and 750 m, the C:S ratios did not change. Because DOC decreased gradually, apparent DOS$_{SPE}$ also decreased gradually. δ^{34}S values decreased significantly (R^2 = 0.32; P < 0.005), while δ^{13}C values did not change. Average δ^{34}S values and C:S ratios were 17.8 ± 0.8‰ and 236 ± 24, respectively. In the bathypelagic samples, between 750 and 5,000 m, none of the parameters showed statistically significant

Table 1. Properties of marine DOM$_{SPE}$ samples binned by depth

Depth range (m)	DOM$_{SPE}$ C:S (molar)	DOM$_{SPE}$ δ^{34}S (‰)	DOM$_{SPE}$ δ^{13}C (‰)	DOC (μM)	DOS (nM)
0–150	213 ± 32	18.6 ± 0.8	−22.4 ± 0.3	62 ± 13	283 ± 66
150–750	236 ± 24	17.8 ± 0.8	−22.2 ± 0.3	46 ± 6	192 ± 33
750–5,000	252 ± 27	17.1 ± 1.1	−22.2 ± 0.3	41 ± 3	163 ± 19

Averages are reported with 1σ SDs.

correlations with depth. Average $\delta^{34}S$ values and C:S ratios in the deepest samples were 17.1 ± 1.1‰ and 252 ± 27, respectively. DOM_{SPE} $\delta^{13}C$ values were constant throughout the water column, with an average of –22.3 ± 0.3‰. DOM_{SPE} $\delta^{34}S$ values also had statistically significant positive correlations with DOC concentration ($R^2 = 0.25$; $P < 0.001$) and, therefore, apparent DOS_{SPE} concentration ($R^2 = 0.38$; $P < 0.001$) and temperature ($R^2 = 0.28$; $P < 0.001$), although all these parameters covaried with depth (*SI Appendix*, Fig. S7).

Discussion

To assess the possible contribution of sulfurized porewater DOS sources to the open ocean using a two-parameter ($\delta^{34}S$, C:S), two-endmember mixing calculation, we first constrained 1) the composition of biotic DOS_{SPE} in the surface ocean, which we defined as the upper 50 m of the water column, and 2) the composition of abiotic DOS_{SPE} in sulfidic porewaters. The results of 1) and 2) allow us to conclude that 3) there is limited isotopic evidence for porewater sources to global marine DOS_{SPE} and more broadly, to DOS and DOM. Finally, we discuss 4) potential mechanisms for observed sulfur isotope heterogeneity with depth.

Composition of Biotic DOS in the Surface Ocean. Primary producers in the photic zone invest energy to transform inorganic sulfate into biomass through assimilatory sulfate reduction (6). Very few studies have examined the consequences of these reactions for the sulfur isotope composition of organic matter in phytoplankton; preliminary measurements of marine algae found that bulk biomass was minimally (by 0.8‰) ^{34}S-depleted from marine sulfate (35), which is a nearly constant 21‰ (36). Further work on phytoplankton dimethylsulfoniopropionate and dimethyl sulfide (DMS) found ^{34}S-depletions from marine sulfate by ∼1–3‰ (37–39). Our dataset of surface DOM_{SPE} $\delta^{34}S$ (<50 m depth) values averaged 18.6 ± 0.6‰, which aligns with these studies and supports the idea that phytoplankton-derived organic sulfur in the surface oceans is only slightly fractionated (by up to ∼3‰) relative to marine sulfate.

There are few studies that have investigated C:S ratios of organic matter from primary producers, but most converge on similar amounts of organic sulfur as phosphorous (i.e., S:P ∼1). Laboratory experiments found cultures of *Synechococcus* incorporating carbon, nitrogen, and sulfur at a ratio of 95:16:1 (40). A study of 15 marine eukaryotic phytoplankton found average stoichiometries for C:N:P:S of 124:16:1:1.3 (41). Meanwhile, suspended marine POS, which is assumed to derive from phytoplankton, has C:N:S ratios of ∼110–187:27:1 in the North Pacific (42–44). Euphotic zone DOM_{SPE} (<50 m depth) C:S ratios in this study were similar, averaging 192 ± 25 and ranging between 153–243. This aligns with previous measurements of DOM_{SPE} C:S ratios, which ranged between 188 and 290 in the upper 100 m of the Eastern Atlantic and Southern Ocean (5). Higher C:S ratios in DOM/POM versus phytoplankton suggest substantial losses of relatively sulfur-rich compounds. This presumably includes volatile species like DMS (C:S = 2), which accounts for 40% of the atmospheric sulfur flux from the ocean (45). In summary, we take our phytoplankton-derived surface DOS_{SPE} endmember to have a $\delta^{34}S$ value of 18.6 ± 0.6‰ and a C:S ratio between 153 and 243.

Composition of Abiotic DOS in Sulfidic Porewater. Porewater sulfide and polysulfides react abiotically with organic functional groups to form new C-S bonds in a process called sulfurization (16). The sulfide derives from dissimilatory sulfate reduction (DSR), which, unlike the assimilatory pathway, strongly fractionates sulfur isotopes and results in porewater sulfide $\delta^{34}S$ values as low as –45‰ (46–48). DOS compounds formed by this pathway are thus also expected to have very low $\delta^{34}S$ values. We analyzed porewater samples from tidal flats with high rates of sulfate reduction and organic matter sulfurization: the mangrove-fringed Caeté Estuary and the North Sea (49–51). Because the magnitude of sulfur isotope fractionation by DSR is generally inversely correlated with the sulfate reduction rate (52, 53), these samples should provide an upper bound on porewater sulfide and thus sulfurized DOS_{SPE} $\delta^{34}S$ values.

Our data provide direct constraints on porewater DOS_{SPE} sulfur isotope compositions and indicate that sulfurization is a major process in these sediments. The $\delta^{34}S$ values of DOM_{SPE} in porewaters ranged from –2.7 to 0.7‰, ^{34}S-depleted by almost 20‰ relative to phytoplankton organic sulfur, but relatively ^{34}S-enriched compared with most porewater H_2S measurements (46, 54). DOM_{SPE} C:S ratios ranged between 18 and 45, with much higher sulfur contents than phytoplankton-derived DOS in the surface ocean. These values align with both laboratory studies that incubated DOM_{SPE} in sulfidic water, finding post-sulfurization C:S ratios ∼15 and previous measurements of North Sea porewaters with a C:S ratio of ∼27 (13). Porewater DOM_{SPE} $\delta^{13}C$ values differed in the Caeté Estuary (–26.9 ± 0.1‰) and the North Sea (–23.3 ± 0.2‰), likely reflecting higher terrestrial influences in the mangrove-fringed estuary. Notably, while terrestrial OS is poorly constrained for $\delta^{34}S$ ratios, C:S values are generally higher (55); therefore, while we see influences of terrestrial carbon, no such inputs of terrestrial sulfur are observed. We therefore assume a sulfidic porewater-derived sedimentary endmember to have a $\delta^{34}S$ value of –2.7 to 0.7‰ with C:S ratios between 18 and 45.

Limited Evidence for Porewater Sources to DOS. Mixing calculations using the $\delta^{34}S$ and C:S ratios for the two-endmember sources described above and the measured $\delta^{34}S$ and C:S ratios of DOM_{SPE} indicate that sulfurized porewater sources cannot contribute more than ∼20% of the DOS_{SPE} in any one sample from our open-marine dataset, and no more than ∼8% on average for the deep-ocean samples (Fig. 4). Given that other processes could also lead to $\delta^{34}S$ depletion (see below) and that our porewater samples are, if anything, more ^{34}S-enriched than sulfurized porewater DOS_{SPE} from typical marine sediments (which have more ^{34}S-depleted sulfides), this calculation represents a very conservative maximum estimate (that is, any value <20% is plausible, including 0%). Only samples from the mangrove-fringed Caeté Estuary were within a range of significant contributions (50–80%) from sulfurized organic matter; however, this contribution appears short-lived, likely due to rapid (i.e., weeks to months) photochemical oxidation of and removal from the DOM_{SPE} pool in the estuary before reaching the open ocean (56). Without more data to examine differences between ocean basins, we are unable to address the long-term accumulation of sulfurized porewater DOS_{SPE}, which is assumed to persist in the ocean over multiple mixing cycles. However, the few deep Atlantic data that we do have do not support this hypothesis, as samples from the Bermuda Atlantic Time-Series (BATS) are more ^{34}S-depleted (Figs. 2 and 3; pink triangles) than those from the (older) deep Pacific Ocean. Thus, we can conclude that marine DOS has a dominantly (>92%) biotic origin, that is, presumably produced by microorganisms in the sunlit surface ocean.

Sulfurization reactions have also been documented to occur within anoxic microenvironments in the pelagic ocean, such as

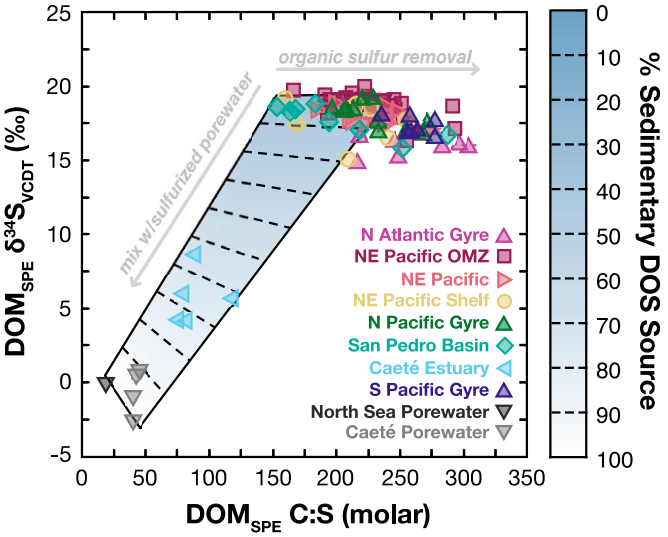

Fig. 4. DOM_{SPE} samples plotted in the same coordinate space and color scheme as Fig. 1*B*, with C:S molar ratios on the *x* axis and $\delta^{34}S$ values on the *y* axis. A linear mixing model is superimposed in the white- to blue-colored polygon, with dashed lines at 10% intervals. Endmembers for the mixing space were inferred from marine surface (<50 m) extracts and porewater samples and are detailed in the discussion. Marine samples have, on average, ~8% DOS contributions from porewater sources and at maximum ~20% (two samples). We hypothesize that heterogeneity in $\delta^{34}S$ values and C:S ratios is a combination of both mixing from porewater sources that lowers $\delta^{34}S$ values, and organic sulfur removal without fractionation that increases C:S ratios (gray arrows). VCDT, Vienna Canyon Diablo Troilite.

sinking particles in OMZs, where genomic studies found active transcription of genes for sulfate reduction (57, 58), and incubation studies with radioactively labeled sulfur confirmed that particulate organic matter sulfurization was occurring (59). It remains uncertain if this process translates from the particulate to the dissolved sulfur pool. Our data from the NE Pacific OMZ ($n = 31$; magenta squares, Figs. 2–4) were collected from adjacent stations to Raven et al. (59) and spanned dissolved O_2 concentrations from 0 to 250 μM. Yet, we observed no significant changes to either C:S ratios or $\delta^{34}S$ values with dissolved oxygen (*SI Appendix*, Fig. S10). This suggests that sulfurization reactions in that anoxic water column minimally or negligibly contribute to marine DOS; globally significant contributions from other, more sulfidic water bodies, seem unlikely (60).

The conclusion that porewater fluxes of sulfurized organic matter do not greatly impact the present marine global DOS inventory was somewhat unexpected, given previous estimates of large benthic fluxes (30-200 Tg sulfur yr^{-1} (13)), which are calculated by dividing DOC fluxes by porewater DOM_{SPE} C:S ratios. There are several potential explanations for this discrepancy, including incorrect estimates of 1) DOM_{SPE} C:S ratios, and/or 2) porewater DOC fluxes. Existing measurements of porewater DOM_{SPE} C:S ratios are highly biased toward porewater samples and environments with known sulfurization—if global average porewater DOM_{SPE} C:S ratios are much higher, then calculated DOS fluxes would decrease. Notably, DOC fluxes are highest in areas with high rates of sulfate reduction (61), i.e., continental margin sediments (121-233 Tg carbon yr^{-1} (62, 63)) and intertidal sediments (106-416 Tg carbon yr^{-1}, ref (64). Given that ~70% of porewater DOC flux is estimated to occur from sediments that have active sulfate reduction, the bias in porewater DOM_{SPE} C:S ratios is likely only minor. Alternatively, calculated DOC fluxes might be overestimated. Our dataset offers a window to sedimentary DOS/DOC fluxes for comparison: Given a conservative maximum of 20% (Fig. 4) of the >6,700 Tg sulfur DOS inventory that was initially estimated to derive from porewater fluxes, and an average lifetime for DOS of ~4,000 y (5) assuming that DOS compounds share the same average radiocarbon age as bulk DOC, the sedimentary flux of DOS to the global ocean is <0.4 Tg sulfur yr^{-1}. Porewater C:S ratios (~10–50) further imply DOC fluxes of 1.6–7.6 Tg carbon yr^{-1}, orders of magnitude below those reported from either intertidal or continental margin sediments. Although it is possible to invoke a DOC flux with little concurrent DOS flux, such a scenario would require C:S ratios >2,500 that are difficult to imagine from areas with active sulfur cycling (and notably, much higher than the highest recorded value of 1,472 (7)). Either sulfurized DOS suffers extreme preferential loss over DOC or porewaters are orders of magnitude less significant sources of marine DOM than previously thought. Finally, if the lifetime of porewater-derived DOS in the water column is significantly shorter than the average radiocarbon age of DOC used above (~4,000 y), then sedimentary porewater fluxes could be higher, but this would mean that porewater DOS does not contribute to the refractory DOM reservoir.

Causes of Spatial $\delta^{34}S$ Heterogeneity in DOM. We next turn to the observed decrease in $\delta^{34}S$ and increase in C:S ratios of DOM_{SPE} with depth (Figs. 2*C* and 3). In shallow (0-150 m depth) waters, the loss of apparent DOS_{SPE} and DOC, increase in C:S ratios, and near-constant $\delta^{34}S$ and $\delta^{13}C$ values with depth can be readily explained by the rapid uptake and/or remineralization of phytoplankton-derived labile DOS compounds without fractionation. The preferential loss of sulfur relative to carbon is similar to that observed for nitrogen and phosphorous over the same depth by other studies (1, 65) and is unsurprising given that a majority of organic sulfur is present as diverse bioavailable components like thiols, sulfonates, or thiophenes (6, 7). The minimal isotopic fractionation also agrees with studies of both specific degradation reactions (38) and bulk trophic level effects (66, 67). In contrast, DOS_{SPE} in the deep ocean is lower in concentration (163 ± 19 versus 283 ± 66 nM), has higher C:S ratio (252 ± 27 versus 213 ± 32), and lower $\delta^{34}S$ value (17.1 ± 1.1‰ versus 18.6 ± 0.8‰; Table 1). Changes in DOS_{SPE} concentration and C:S ratios can be explained as the continuous degradation of semilabile and semirefractory compounds. The lower $\delta^{34}S$ values of deep water DOM_{SPE} cannot, however, be easily explained by a simple degradation model (Fig. 4) because the shift is in the opposite direction of that expected from a normal isotope effect.

Strong intramolecular heterogeneity in $\delta^{34}S$ of DOS_{SPE} compounds could potentially yield the observed isotopic patterns if the DOS_{SPE} that is removed with depth is significantly ^{34}S-enriched, relative to the remaining DOS_{SPE}. For example, modeling studies and initial data hint that semilabile, reduced organic sulfur compounds like amino acids are more ^{34}S-enriched relative to more recalcitrant, oxidized organic sulfur (26, 55). However, at present there is little direct compound-specific sulfur isotope data to either support or reject this hypothesis. Generation of DOS compounds via the hydrolysis of sinking particles could leave POS ^{34}S-enriched and DOS_{SPE} ^{34}S-depleted, but such a scenario would require large isotope fractionations or active turnover of a large proportion of the deep DOS pool. Finally, addition of terrestrial DOS (generally high in C:S and lower in $\delta^{34}S$) to the deep ocean could explain lower $\delta^{34}S$ with depth but is inconsistent with our nearly invariant $\delta^{13}C$ values (Fig. 3*C*).

Alternatively, deep-ocean DOS_{SPE} could simply be ^{34}S-depleted due to mixing with porewater sulfurized compounds, as discussed above. While this should add S-rich compounds that lower the

C:S ratios, the large $\delta^{34}S$ contrast between surface and porewater DOS_{SPE} means that the isotopic composition is much more sensitive to this addition than the elemental ratio (Fig. 4). If this mechanistic explanation is correct, the trends of decreasing apparent DOS, increasing C:S ratios, and decreasing $\delta^{34}S$ values observed in intermediate-depth waters can be understood as the superposition of two processes (Fig. 4, gray arrows). Thus, we hypothesize that C:S ratios of DOM_{SPE} increase with depth (up to ~750 m) due to mixing with older water masses and concurrent slow degradation, but without appreciable isotopic fractionation. Meanwhile, the $\delta^{34}S$ of deep DOS_{SPE} is lower due to the addition of small amounts of ^{34}S-depleted sulfurized DOM_{SPE} from porewaters and possibly other sources.

Conclusions. We developed an improved (~10x more sensitive for sulfur) analytical measurement for marine DOM_{SPE}, enabling concurrent measurements of $\delta^{34}S$ values, $\delta^{13}C$ values, and C:S ratios on ~350 μg DOM_{SPE}. We used this technique to produce a global survey of marine DOM_{SPE} $\delta^{34}S$ values and show that abiotically sulfurized organic matter from sulfidic porewater is on average <8% of the marine DOS_{SPE} pool. As this is a conservative upper bound, we conclude that sulfurized porewater DOS is only a small component of the oceanic DOM inventory. The accumulation of refractory, sulfurized porewater is therefore not a main process that could explain the old radiocarbon ages of oceanic DOM_{SPE}. Instead, DOS apparently derives mostly from biological assimilation of sulfate in the sunlit surface ocean. Trends of increasing C:S ratios and decreasing $\delta^{34}S$ values with depth could reflect the continuous removal of surface-derived DOM_{SPE} superimposed on a background of this small inventory of sulfurized DOS_{SPE}.

Materials and Methods

Sample Collection. DOM_{SPE} samples were collected between 2016 and 2021 on 10 cruises (see *SI Appendix* for details), including the BATS and the Hawaii Ocean Time-Series, that covered the following regions: N Pacific Gyre, N Atlantic Gyre, S Pacific Gyre, NE Pacific, NE Pacific Shelf, NE Pacific OMZ, San Pedro Basin (coastal California), and the Caeté Estuary (Amazonian mangroves). Porewater DOM_{SPE} samples were collected from the intertidal sediments of the mangrove-fringed Caeté Estuary, south of the Amazon Estuary in North Brazil, and a North Sea intertidal flat in Germany. For marine samples, conductivity, temperature, and density casts for physical parameters (i.e., dissolved oxygen, salinity, fluorescence, temperature) were taken at each station and can be found in the *SI Appendix* (*SI Appendix*, Figs. S1–S7). Seawater (~5–20 L samples) was collected from Niskin bottles into acid-washed polyethylene containers and filtered through a 0.80/0.45 μm capsule filter (AcroPak 500) prior to acidification to pH 2 with reagent grade 12 N hydrochloric acid. DOC concentrations were measured prior to SPE via high-temperature combustion on a Shimadzu Total Organic Carbon Analyzer (Shimadzu Corp). Nutrients (nitrate, phosphate, and silicate) were measured via colorimetry on an AutoAnalyzer II (Seal Analytical; see *SI Appendix* for station-specific methods details and references).

DOM_{SPE} Isolation. DOM_{SPE} was concentrated using SPE with Bond Elute PPL cartridges (Agilent; 1 g, 6 mL size) following Dittmar et al. (28). DOM_{SPE} samples were eluted in GC-grade methanol (28). Extracts were dried under a stream of N_2 gas and transferred to 2 mL GC vials and then to 150 μL glass inserts. Aliquots corresponding to ~4.5 μg sulfur (~350 μg DOC) were transferred in methanol from 2 mL GC vials into smooth-walled tin EA capsules (6 × 2.9 mm, OEA Laboratories). Methanol was evaporated at room temperature (~2 h) prior to folding.

EA-IRMS Measurements. Tin capsules containing dried DOM_{SPE} were folded closed, loaded into an autosampler, and then combusted and analyzed in a Thermo Scientific EA IsoLink IRMS System for determination of C:S molar ratios, $\delta^{34}S$ values, and $\delta^{13}C$ values. The system comprised a Flash combustion EA coupled to a Delta V Plus IRMS via a ConFlo IV Universal Interface. Carbon and sulfur isotope analysis and data processing followed a previously published method (26). Due to the high C:S molar ratios of DOM_{SPE}, CO_2 was diluted by 88.4% following combustion via the ConFlo. Urea standards were run at the same settings to account for any possible fractionation of ^{13}C by this dilution. Sulfur isotope and concentration standards included a methionine working standard, seawater sulfate, and silver sulfide reference materials (IAEA S1, S2, S3). Additionally, a working standard of DOM_{SPE} extracted in a large batch (~200 L) from the Scripps Institution of Oceanography (SIO) pier was run in at least triplicate with each sample set. Sample $\delta^{34}S$ values were corrected for linearity (peak height) effects and then calibrated to IAEA reference materials. sulfur content (<0.10 μg sulfur) and $\delta^{34}S$ values (~8‰) of tin capsules were also measured by EA-IRMS and used to correct subsequent analyses for the blank contribution (68). $\delta^{34}S$ values are reported as permil (‰) variations relative to the Vienna Canyon Diablo Troilite reference frame, while $\delta^{13}C$ values are reported relative to Vienna Pee Dee Belemnite. C:S ratios were obtained by dividing corrected carbon and sulfur amounts (molar ratio), as calculated from EA peak areas. Extracts supplied by collaborators were often limited by sample size to single or duplicate analyses, so we could not estimate precision directly for each sample. Instead, uncertainties in isotopic compositions and C:S ratios for samples are reported using the SD of our DOM_{SPE} SIO pier standard measurements, divided by the square root of sample replicates analyzed. These SEs (1σ) were ≤0.2‰ for $\delta^{34}S$ values and $\delta^{13}C$ values and ≤6 for C:S ratios. DOS_{SPE} concentrations were calculated as the product of measured total DOC concentration and DOM_{SPE} C:S ratio, and we therefore refer to DOS_{SPE} concentrations as "apparent" throughout.

Sulfate Carryover. We also considered the carryover of seawater sulfate in DOM_{SPE} extracts as a potential source of systematic error. Blank extractions using 28 mM Na_2SO_4 in deionized water on the PPL SPE cartridges showed no measurable sulfur above the capsule blank (0.10 μg sulfur) via EA-IRMS. Taking this as the upper limit for sulfate blank, and assuming a $\delta^{34}S$ value of +21‰ (36), we calculated a worst-case error (for a sample with just 1 μg sulfur and measured $\delta^{34}S$ of 15‰) of 0.6‰. For a sulfate blank half that size, and a more typical sample of 4 μg sulfur and $\delta^{34}S = 17.5$‰, the effect would be just 0.05‰. There was no correlation between SO_2 peak size in the EA and measured $\delta^{34}S$ ($R^2 = 0.0004$), so we conclude that sulfate contamination is very unlikely to have caused either the relative ^{34}S enrichments or the depth-related trends in our dataset. DOM_{SPE} samples with peak sizes that corresponded to <1 μg sulfur were not reported to further minimize any possibility of blank-related artifacts.

Data, Materials, and Software Availability. All study data are included in the article and/or supporting information.

ACKNOWLEDGMENTS. We thank the crew, administrative teams, and science parties of the *R/V Atlantic Explorer* and the *R/V Kilo Moana* for their assistance during the Bermuda Atlantic Time-Series and Hawaii Ocean Time-Series cruises, especially Rod Johnson and Carolina Funkey. We thank Daniela Osorio Rodriguez and Sijia Dong for their assistance in sample collection aboard the *R/V Sally Ride* andJess Adkins from Caltech. We thank Troy Gunderson from the San Pedro Ocean Time-Series and the crew of the *R/V Yellowfin*. We acknowledge Mike Beman for inviting our participation on cruises that provided the NE Pacific OMZ samples and Ken Smith for supporting the acquisition of the Station M NE Pacific samples. We are grateful to members and technicians in the Aluwihare Lab at Scripps Institution of Oceanography, especially Brandon Stephens, Irina Koester, and Tran Nguyen. We acknowledge Usha Lingappa for drafting Figure 1. We thank colleagues for early reviews and conversations about the manuscript, including Tony Wang, Hannah Dion-Kirschner, Morgan Raven, and Ted Present, and other members of the Adkins and Sessions Labs at Caltech. We thank University of California Santa Cruz Professor Matthew McCarthy for early conversations and support for the project. Color-blind-friendly palettes were generated from Paul Tol's online resource. Funding for this work was provided by NSF OCE (Division of Ocean Sciences) Grant 2023676 to A.L.S. and A.A.P.; M.S. and T.D. acknowledge funding by the DFG-FAPERJ (German Research Foundation) cooperative project (DI 842/6-1) and within the Cluster of Excellence EXC 2077 "The Ocean Floor - Earth's Uncharted Interface" (DFG Project number

390741603). P.C.K. is grateful for funding from the Cohan-Jacobs and Stein Families Fellowship of the Fannie and John Hertz Foundation. Portions of this work were developed from the 2021 doctoral dissertation of Alexandra A Phillips at Caltech.

Author affiliations: [a]Division of Geological and Planetary Sciences, California Institute of Technology, Pasadena, CA 91125; [b]Scripps Institution of Oceanography, University of California San Diego, La Jolla, CA 92093; [c]Institute for Chemistry and Biology of the Marine Environment, University of Oldenburg, 26129, Oldenburg, Germany; [d]University of Southern California, Los Angeles, CA 90007; and [e]Helmholtz Institute for Functional Marine Biodiversity, University of Oldenburg, 26129 Oldenburg, Germany

1. D. Hansell, C. Carlson, D. Repeta, R. Schlitzer, Dissolved organic matter in the ocean: A controversy stimulates new insights. *Oceanog.* **22**, 202–211 (2009).
2. P. M. Williams, E. R. M. Druffel, Radiocarbon in dissolved organic matter in the central North Pacific Ocean. *Nature* **330**, 246–248 (1987).
3. D. A. Hansell, Recalcitrant dissolved organic carbon fractions. *Annu. Rev. Mar. Sci.* **5**, 421–445 (2013).
4. M. Stuiver, P. D. Quay, H. G. Ostlund, Abyssal water carbon-14 distribution and the age of the world oceans. *Science* **219**, 849–851 (1983).
5. K. B. Ksionzek *et al.*, Dissolved organic sulfur in the ocean: Biogeochemistry of a petagram inventory. *Science* **354**, 456–459 (2016).
6. M. A. Moran, B. P. Durham, Sulfur metabolites in the pelagic ocean. *Nat. Rev. Microbiol.* **17**, 665–678 (2019).
7. K. Longnecker, L. Oswald, M. C. K. Soule, G. A. Cutter, E. B. Kujawinski, Organic sulfur: A spatially variable and understudied component of marine organic matter. *Limnol. Oceanogr. Lett.* **5**, 305–312 (2020).
8. D. S. Smith, R. A. Bell, J. R. Kramer, Metal speciation in natural waters with emphasis on reduced sulfur groups as strong metal binding sites. *Comp. Biochem. Physiol. C Toxicol. Pharmacol.* **133**, 65–74 (2002).
9. P. A. Matrai, R. D. Vetter, Particulate thiols in coastal waters: The effect of light and nutrients on their planktonic production. *Limnol. Oceanogr.* **33**, 624–631 (1988).
10. R. al-Farawati, C. M. Van Den Berg, Thiols in coastal waters of the western North Sea and English Channel. *Environ. Sci. Technol.* **35**, 1902–1911 (2001).
11. C. L. Dupont *et al.*, Genomic insights to SAR86, an abundant and uncultivated marine bacterial lineage. *ISME J.* **6**, 1186–1199 (2012).
12. H. J. Tripp *et al.*, SAR11 marine bacteria require exogenous reduced sulphur for growth. *Nature* **452**, 741–744 (2008).
13. A. M. Pohlabeln, G. V. Gomez-Saez, B. E. Noriega-Ortega, T. Dittmar, Experimental evidence for abiotic sulfurization of marine dissolved organic matter. *Front. Mar. Sci.* **4**, 1–11 (2017).
14. L. Shawar *et al.*, Dynamics of pyrite formation and organic matter sulfurization in organic-rich carbonate sediments. *Geochim. Cosmochim. Acta* **241**, 219–239 (2018).
15. J. P. Werne, D. J. Hollander, T. W. Lyons, J. S. Sinninghe Damsté, "Organic sulfur biogeochemistry: Recent advances and future research directions" in *Sulfur Biogeochemistry - Past and Present* (Geological Society of America, 2004). pp. 135–150.
16. M. E. L. Kohnen, J. S. S. Damsté, H. L. ten Haven, J. W. de Leeuw, Early incorporation of polysulphides in sedimentary organic matter. *Nature* **341**, 640–641 (1989).
17. J. S. Sinninghe Damsté, M. D. Kok, J. Köster, S. Schouten, Sulfurized carbohydrates: An important sedimentary sink for organic carbon? *Earth Planet. Sci. Lett.* **164**, 7–13 (1998).
18. M. Boussafir, E. Lallier-Verges, Accumulation of organic matter in the Kimmeridge Clay formation (KCF): An update fossilisation model for marine petroleum source-rocks. *Mar. Pet. Geol.* **14**, 75–83 (1997).
19. M. Boussafir *et al.*, Electron microscopy and pyrolysis of kerogens from the Kimmeridge Clay Formation, UK: Source organisms, preservation processes, and origin of microcycles. *Geochim. Cosmochim. Acta* **59**, 3731–3747 (1995).
20. M. R. Raven *et al.*, Organic carbon burial during OAE2 driven by changes in the locus of organic matter sulfurization. *Nat. Commun.* **9**, 3409 (2018).
21. J. de Leeuw, J. Sinninghe-Damste, Organic sulfur compounds and other biomarkers as indicators of palaeosalinity. *ACS Symp. Ser.* **429**, 417–443 (1990).
22. K. Grice *et al.*, Structural and isotopic analysis of kerogens in sediments rich in free sulfurised *Botryococcus braunii* biomarkers. *Org. Geochem.* **34**, 471–482 (2003).
23. K. M. Meyer, L. R. Kump, Oceanic euxinia in earth history: Causes and consequences. *Annu. Rev. Earth Planet. Sci.* **36**, 251–288 (2008).
24. H. A. Abdulla, D. J. Burdige, T. Komada, Abiotic formation of dissolved organic sulfur in anoxic sediments of Santa Barbara Basin. *Org. Geochem.* **139**, 103879 (2020).
25. T. Dittmar, "Chapter 7 - Reasons behind the long-term stability of dissolved organic matter" in *Biogeochemistry of Marine Dissolved Organic Matter*, D. A. Hansell, C. A. Carlson, Eds. (Academic Press, ed. 2, 2015), pp. 369–388.
26. A. A. Phillips, F. Wu, A. L. Sessions, Sulfur isotope analysis of cysteine and methionine via preparatory liquid chromatography and elemental analyzer isotope ratio mass spectrometry. *Rapid Commun. Mass Spectrom.* **35**, e9007 (2021).
27. E. R. M. Druffel, P. M. Williams, Importance of isotope measurements in marine organic geochemistry. *Mar. Chem.* **39**, 209–215 (1992).
28. T. Dittmar, B. Koch, N. Hertkorn, G. Kattner, A simple and efficient method for the solid-phase extraction of dissolved organic matter (SPE-DOM) from seawater. *Limnol. Oceanogr. Methods* **6**, 230–235 (2008).
29. C. Torrentó *et al.*, Solid-phase extraction method for stable isotope analysis of pesticides from large volume environmental water samples. *Analyst (Lond.)* **144**, 2898–2908 (2019).
30. S. N. Silverman *et al.*, Practical considerations for amino acid isotope analysis. *Org. Geochem.* **164**, 104345 (2022).
31. O. Rach, X. Hadeen, D. Sachse, An automated solid phase extraction procedure for lipid biomarker purification and stable isotope analysis. *Org. Geochem.* **142**, 103995 (2020).
32. A. Amrani, A. L. Sessions, J. F. Adkins, Compound-specific δ34S analysis of volatile organics by coupled GC/multicollector-ICPMS. *Anal. Chem.* **81**, 9027–9034 (2009).
33. T. Broek, B. Walker, T. Guilderson, M. McCarthy, Coupled ultrafiltration and solid phase extraction approach for the targeted study of semi-labile high molecular weight and refractory low molecular weight dissolved organic matter. *Mar. Chem.* **194**, 146–157 (2017).
34. W. M. Johnson, M. C. Kido Soule, E. B. Kujawinski, Extraction efficiency and quantification of dissolved metabolites in targeted marine metabolomics. *Limnol. Oceanogr. Methods* **15**, 417–428 (2017).
35. I. R. Kaplan, K. O. Emery, S. C. Rittenberg, The distribution and isotopic abundance of sulphur in recent marine sediments off southern California. *Geochim. Cosmochim. Acta* **27**, 297–331 (1963).
36. G. Paris, A. L. Sessions, A. V. Subhas, J. F. Adkins, MC-ICP-MS measurement of δ 3 4 S and Δ 3 3 S in small amounts of dissolved sulfate. *Chem. Geol.* **345**, 50–61 (2013).
37. H. Oduro, K. L. Van Alstyne, J. Farquhar, Sulfur isotope variability of oceanic DMSP generation and its contributions to marine biogenic sulfur emissions. *Proc. Natl. Acad. Sci. U.S.A.* **109**, 9012–9016 (2012).
38. D. Osorio-Rodriguez *et al.*, Sulfur isotope fractionations constrain the biological cycling of dimethylsulfoniopropionate in the upper ocean. *Limnol. Oceanogr.* **66**, 3607–3618 (2021).
39. A. Amrani, W. Said-Ahmad, Y. Shaked, R. P. Kiene, Sulfur isotope homogeneity of oceanic DMSP and DMS. *Proc. Natl. Acad. Sci. U.S.A.* **110**, 18413–18418 (2013).
40. R. L. Cuhel, J. B. Waterbury, Biochemical composition and short term nutrient incorporation patterns in a unicellular marine cyanobacterium, Synechococcus (WH 7 8 0 3) 1. *Limnol. Oceanogr.* **29**, 370–374 (1984).
41. T.-Y. Ho *et al.*, The elemental composition of some marine phytoplankton1. *J. Phycol.* **39**, 1145–1159 (2003).
42. P. A. Matrai, R. W. Eppley, Particulate organic sulfur in the waters of the Southern California Bight. *Global Biogeochem. Cycles* **3**, 89–103 (1989).
43. T. S. Bates *et al.*, The cycling of sulfur in surface seawater of the northeast Pacific. *J. Geophys. Res. Oceans* **99**, 7835–7843 (1994).
44. M. R. Raven, R. G. Keil, S. M. Webb, Rapid, concurrent formation of organic sulfur and iron sulfides during experimental sulfurization of sinking marine particles. *Global Biogeochem. Cycles* **35**, e2021GB007062 (2021).
45. A. Lana *et al.*, An updated climatology of surface dimethlysulfide concentrations and emission fluxes in the global ocean: Updated DMS climatology. *Global Biogeochem. Cycles* **25**, 21–17 (2011).
46. H. G. Thode, J. Macnamara, W. H. Fleming, Sulphur isotope fractionation in nature and geological and biological time scales. *Geochim. Cosmochim. Acta* **3**, 235–243 (1953).
47. K. S. Habicht, D. E. Canfield, Isotope fractionation by sulfate-reducing natural populations and the isotopic composition of sulfide in marine sediments. *Geology* **29**, 555–558 (2001).
48. M. S. Sim, T. Bosak, S. Ono, Large sulfur isotope fractionation does not require disproportionation. *Science* **333**, 74–77 (2011).
49. A. Kamyshny, T. Ferdelman, Dynamics of zero- valent sulfur species including polysulfides at seep sites on intertidal sand flats (Wadden Sea, North Sea). *Mar. Chem.* **121**, 17–26 (2010).
50. M. Seidel *et al.*, Biogeochemistry of dissolved organic matter in an anoxic intertidal creek bank. *Geochim. Cosmochim. Acta* **140**, 418–434 (2014).
51. M. R. Raven, D. A. Fike, M. L. Gomes, S. M. Webb, Chemical and isotopic evidence for organic matter sulfurization in redox gradients around mangrove roots. *Front. Earth Sci.* **7**, 1–15 (2019).
52. A. S. Bradley, W. D. Leavitt, D. T. Johnston, Revisiting the dissimilatory sulfate reduction pathway. *Geobiology* **9**, 446–457 (2011).
53. B. A. Wing, I. Halevy, Intracellular metabolite levels shape sulfur isotope fractionation during microbial sulfate respiration. *Proc. Natl. Acad. Sci. U.S.A.* **111**, 18116–18125 (2014).
54. D. E. Canfield, Biogeochemistry of sulfur isotopes. *Rev. Mineral. Geochem.* **43**, 607–636 (2001).
55. G. Tcherkez, I. Tea, 3 2 S / 3 4 S isotope fractionation in plant sulphur metabolism. *New Phytol.* **200**, 44–53 (2013).
56. G. V. Gomez-Saez, A. M. Pohlabeln, A. Stubbins, C. M. Marsay, T. Dittmar, Photochemical alteration of dissolved organic sulfur from sulfidic porewater. *Environ. Sci. Technol.* **51**, 14144–14154 (2017).
57. M. W. Smith, L. Zeigler Allen, A. E. Allen, L. Herfort, H. M. Simon, Contrasting genomic properties of free-living and particle-attached microbial assemblages within a coastal ecosystem. *Front. Microbiol.* **4**, 1–20 (2013).
58. M. T. Carolan, J. M. Smith, J. M. Beman, Transcriptomic evidence for microbial sulfur cycling in the eastern tropical North Pacific oxygen minimum zone. *Front. Microbiol.* **6**, 334 (2015).
59. M. R. Raven, R. G. Keil, S. M. Webb, Microbial sulfate reduction and organic sulfur formation in sinking marine particles. *Science* **371**, 178–181 (2020).
60. G. V. Gomez-Saez *et al.*, Sulfurization of dissolved organic matter in the anoxic water column of the Black Sea. *Sci. Adv.* **7**, eabf6199 (2021).
61. B. B. Jørgensen, A. J. Findlay, A. Pellerin, The biogeochemical sulfur cycle of marine sediments. *Front. Microbiol.* **10**, 849 (2019).
62. D. J. Burdige, Preservation of organic matter in marine sediments: Controls, mechanisms, and an imbalance in sediment organic carbon budgets? *Chem. Rev.* **107**, 467–485 (2007).
63. D. J. Burdige, T. Komada, "Sediment pore waters" in *Biogeochemistry of Marine Dissolved Organic Matter* (Elsevier, 2015), pp. 535–577.
64. D. T. Maher, B. D. Eyre, Benthic fluxes of dissolved organic carbon in three temperate Australian estuaries: Implications for global estimates of benthic DOC fluxes. *J. Geophys. Res. Biogeosci.* **115**, 1–15 (2010).
65. C. S. Hopkinson Jr., J. J. Vallino, Efficient export of carbon to the deep ocean through dissolved organic matter. *Nature* **433**, 142–145 (2005).
66. B. J. Peterson, R. W. Howarth, R. H. Garritt, Multiple stable isotopes used to trace the flow of organic matter in estuarine food webs. *Science* **227**, 1361–1363 (1985).
67. B. J. Peterson, B. Fry, Stable isotopes in ecosystem studies. *Annu. Rev. Ecol. Syst.* **18**, 293–320 (1987).
68. J. M. Hayes, Fractionation of the isotopes of carbon and hydrogen in biosynthetic processes. *Stable Isotope Geochemistry*, **43**, 225–277 (2001).